IEEE Photonics Journal
An IEEE Photonics Society Publication

Open Access

Exploring High Quality Chaotic Signal Generation in a Mutually Delay Coupled Semiconductor Lasers System

Volume 9, Number 5, October 2017

Yu-Shuang Hou
Li-Lin Yi
Guang-Qiong Xia
Zheng-Mao Wu

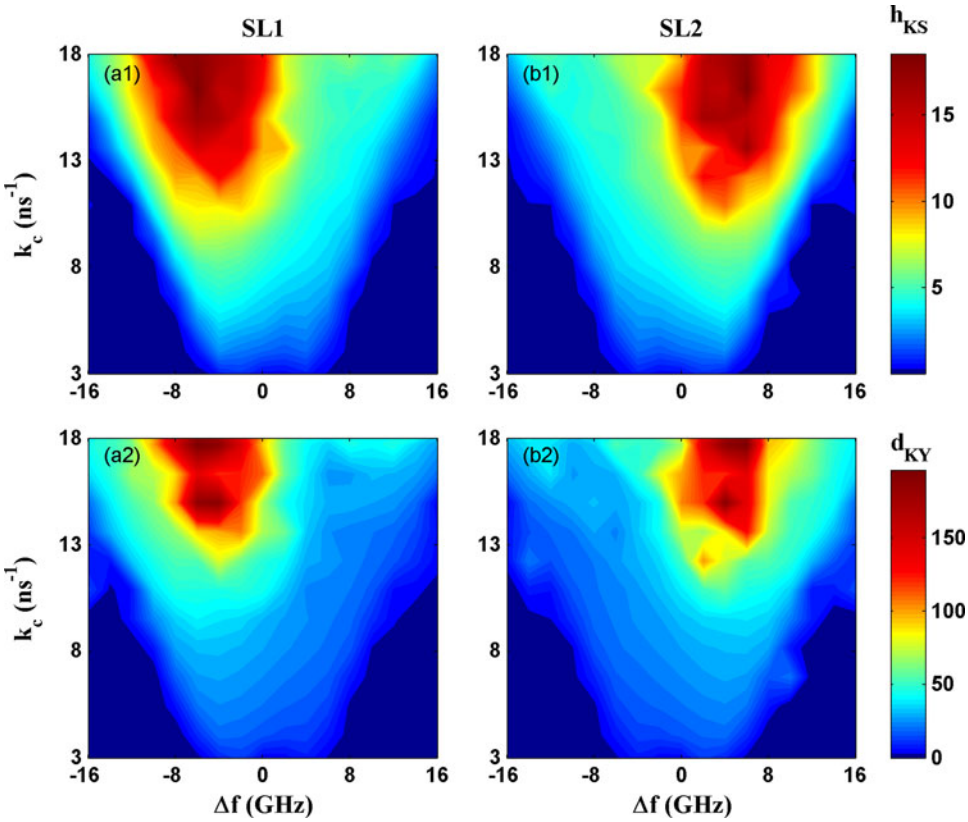

DOI: 10.1109/JPHOT.2017.2737561
1943-0655 © 2017 IEEE

IEEE photonics SOCIETY

IEEE

Exploring High Quality Chaotic Signal Generation in a Mutually Delay Coupled Semiconductor Lasers System

Yu-Shuang Hou,[1,2] Li-Lin Yi,[3] Guang-Qiong Xia,[1] and Zheng-Mao Wu[1]

[1]School of Physical Science and Technology, Southwest University, Chongqing 400715, China
[2]School of Science, Inner Mongolia University of Science and Technology, Baotou 014010, China
[3]State Key Lab of Advanced Communication Systems and Networks, Shanghai Jiao Tong University, Shanghai 200240, China

DOI:10.1109/JPHOT.2017.2737561

Manuscript received June 27, 2017; revised July 31, 2017; accepted August 5, 2017. Date of publication August 8, 2017; date of current version August 28, 2017. This work was supported by the National Natural Science Foundation of China under Grants 61475127 and 61575163. Corresponding authors: Guang-Qiong Xia and Zheng-Mao Wu (e-mail: gqxia@swu.edu.cn; zmwu@swu.edu.cn).

Abstract: High quality chaotic signal generation in a mutually delay coupled semiconductor lasers (MDC-SLs) system is numerically explored by evaluating the time-delay signature (TDS) and complexity of chaotic signals. Autocorrelation function is utilized for quantitatively identifying the TDS of chaotic signal, and Kolmogorov–Sinai entropy and Kaplan–York dimensions are applied to estimate the complexity of chaotic signal. The results show that, under suitable parameters, two sets of chaotic signals with weak TDS and high complexity can be obtained simultaneously. By analyzing the influences of the mutual coupling strength and frequency detuning between the two MDC-SLs on the TDS and complexity of chaotic signals, the optimized parameter regions are specified for simultaneously generating two sets of high quality chaotic signals based on the MDC-SLs system.

Index Terms: Mutually delay coupled semiconductor lasers, optical chaos, time-delay signature, complexity.

1. Introduction

Optical chaos has attracted extensive attention for its potential applications in secure optical communication [1]–[4], fast physical random number (PRN) generation [5]–[8], chaotic lidar [9], logic gate [10] and so on. Since semiconductor lasers (SLs) can be readily driven into chaotic state under additionally external perturbation such as optical injection (OI), optical feedback (OF), and optoelectronic feedback (OEF), the SL under external perturbation is one of the most commonly used chaotic source. Among these external perturbations, the time delayed feedback (OF or OEF) is more desirable for generating higher complex degree chaotic signal. However, chaotic signals generated by such a time-delay system usually contain obvious time-delay signature (TDS) [11], [12], which is undesirable in some special application scenarios. For example, in optical chaos secure communications, the chaotic carrier may be reconstructed by eavesdroppers via chaos analysis technique once the TDS is extracted [13], and then the security of system will be threaten. For fast

Fig. 1. Schematic of a MDC-SLs system. VA: variable attenuator.

physical random number (PRN) generation, the TDS induces recurrence features and then partly affects the statistical performance [6], [14]. Therefore, in order to obtain high quality chaotic signal, the first step is to eliminate the TDS of chaotic signal generated by the SL-based time-delayed feedback system.

So far, much effort has been focused on hiding the TDS of chaotic signals [11], [12], [15]–[26]. For typical single optical feedback (SOF) SL system, Rontani *et al.* demonstrated that when the feedback rate is moderate and the injection current set such that the laser relaxation-oscillation period is close to the delayed time, the time-delay identification becomes extremely difficult [11], [12]. For double optical feedback (DOF) SL systems, Lee *et al.* pointed out that, the TDS cannot be extracted accurately if the length of the two feedback cavities is fractional [18]. Our group also has experimentally and numerically investigated the TDS of chaos in SOF and DOF SL systems [22]–[24]. In particular, we use another SL as a nonlinear active optical feedback device to construct a mutually delay coupled semiconductor lasers (MDC-SLs) system, and investigate the TDS concealment of chaotic signals [25], [26]. Such MDC-SLs system possesses the superiority for simultaneously generating two sets of chaotic signals, which can be used for multi-channel PRN generation [7].

Besides TDS, the complexity is another important index to assess the quality of generated chaotic signal, which is vital to some practical applications [14], [27]–[32]. For chaos-based secure communication, an eavesdropper can reconstruct easily the chaotic attractor and make predictability of the message if the chaotic carrier possesses low complexity [28]. For chaos-based PRN generation, chaotic entropy with low complexity results in the generated PRN with low-randomness [14]. Therefore, the chaotic signal with high complexity will be essential.

Based on above analysis together with physical complication of MDC-SLs system and its chaos related applications, in this work, we will devote to explore high quality chaotic signal generation with weak TDS and high complexity in MDC-SLs systems. Here, the used SLs are assumed to be single-mode distributed feedback semiconductor lasers (DFB-SLs). First, based on the rate equations for SLs in a MDC-SLs system, the time series outputs from two SLs can be numerically simulated via MATLAB. Second, the maximum Lyapunov exponent (MLE), which is one of the most important measures for the stability of nonlinear dynamical systems, is utilized to judge the dynamical state of SLs, and then the parameter space composed of the mutual coupling strength and frequency detuning between the two SLs is determined for simultaneously generating two sets of chaotic signals. Next, through calculating autocorrelation function (ACF) of the two chaotic signals, the parameters scope for generating two sets of chaotic signals with weak TDS is further determined. Finally, through adopting high reliability Kolmogorov-Sinai (KS) entropy and Kaplan-Yorke (KY) dimension to evaluate the complexity of the chaotic signals based on Lyapunov spectrum analysis [33], the optimal parameter region for generating two sets high-quality chaotic signals with both weak TDS and high complexity is specified.

2. System Model and Theory

Fig. 1 shows the schematic of a MDC-SLs system. In such system, the adopted SLs are distributed feedback SLs (DFB-SLs), and the mutually coupling strength between them can be controlled by a variable attenuator (VA).

Based on the Lang-Kobayashi rate equations, the rate equations for SLs in a MDC-SLs system can be described by [34]:

$$\frac{dE_1}{dt} = \frac{1}{2}(1+i\alpha_1)\left[\frac{g_1\left(N_1(t)-N_0\right)}{1+\varepsilon E_1(t)^2} - \frac{1}{\tau_p}\right]E_1(t) + \frac{\mathrm{k}}{\tau_L}E_2\left(t-\tau\right)e^{-i2\pi(f_2\tau+\Delta ft)} \tag{1}$$

$$\frac{dE_2}{dt} = \frac{1}{2}(1+i\alpha_2)\left[\frac{g_2\left(N_2(t)-N_0\right)}{1+\varepsilon E_2(t)^2} - \frac{1}{\tau_p}\right]E_2(t) + \frac{\mathrm{k}}{\tau_L}E_1\left(t-\tau\right)e^{-i2\pi(f_1\tau-\Delta ft)} \tag{2}$$

$$\frac{dN_{1,2}}{dt} = J - \frac{N_{1,2}(t)}{\tau_N} - \frac{g_{1,2}\left(N_{1,2}(t)-N_0\right)}{1+\varepsilon E_{1,2}(t)^2}\left|E_{1,2}(t)\right|^2 \tag{3}$$

where subscripts 1 and 2 stand for SL1 and SL2, respectively. E is the slowly varying complex electrical field amplitude, and J is the injection carrier rate. N is the carrier density, and N_0 is the carrier density at transparency. α is the linewidth enhancement factor, g is differential gain coefficient, and ε is the gain saturation coefficient. τ_N is carrier lifetime, and τ_p is the photon lifetime. τ_L is the round-trip time in internal cavity, and τ is the delayed coupling time. k is the coupling coefficient, and k/τ_L is the mutual coupling strength (k_c). f is the frequency for free-running laser, and $\Delta f(=f_1-f_2)$ is the frequency detuning between the two SLs.

Autocorrelation function (ACF) is adopted to identify the TDS of chaotic time series in this work, which is described as follows [11], [12]

$$C(t) = \frac{\left\langle\left(I\left(t+\Delta t\right)-\left\langle I\left(t\right)\right\rangle\right)\left(I\left(t\right)-\left\langle I\left(t\right)\right\rangle\right)\right\rangle}{\sqrt{\left\langle I\left(t\right)-\left\langle I\left(t\right)\right\rangle\right\rangle^2\left\langle I\left(t+\Delta t\right)-\left\langle I\left(t\right)\right\rangle\right\rangle^2}} \tag{4}$$

where $I(t) = |E(t)|^2$, $<\bullet>$ represents time average, and Δt is the lag time.

The complexity in dynamical systems can be analyzed with different techniques such as statistical complexity [35], [36], permutation entropy [37]–[39], non-triviality measure [40], correlation dimension [41], Kolmogorov-Sinai (KS) entropy [27], [33], [42] and Kaplan-Yorke (KY) dimension [27], [33], most of which are based on statistical measurement of time series analysis using observed data that includes undesirable noise. However, KS entropy and KY dimension, which are measured methods of complexity based on Lyapunov spectrum analysis, maybe more reliable since the complexity can be obtained through integrating the linearized rate equations of SLs. As pointed out in [27], [33], KS entropy indicates the divergence of tiny errors on a chaotic trajectory in a multidimensional phase space, and meanwhile KY dimension characterizes the minimum degree of freedom to describe the dynamics of system. In the following discussion, the complexity will be evaluated through calculating both KS entropy and KY dimension.

In order to calculate KS entropy and KY dimension, Lyapunov spectrum should be obtained firstly. For a time-delayed system, there exist many Lyapunov exponents (LEs). All the LEs are ordered from the largest to the lowest values, that is, $\lambda_1 \geq \lambda_2 \geq \ldots \geq \lambda_m \geq \ldots$, and the set of LEs ($\lambda_1, \lambda_2, \ldots, \lambda_m, \ldots$) is named as Lyapunov spectrum. Based on the Lyapunov spectrum, KS entropy and KY dimension can be calculated. KS entropy is estimated from the sum of all the positive LEs [27], [33],

$$h_{KS} = \sum_{m|\lambda_m>0} \lambda_m \tag{5}$$

and KY dimension is calculated from the Lyapunov spectrum [27], [33],

$$d_{KY} = j + \frac{\sum_{i=1}^{j}\lambda_i}{\left|\lambda_{j+1}\right|} \tag{6}$$

TABLE 1
Parameter Definitions and Values Used in Simulations [33]

Parameter	Description	Value
A	Linewidth enhancement factor	5
G	differential gain coefficient	8.4×10^{-13} m^3s^{-1}
E	gain saturation coefficient	2.5×10^{-23}
N_0	carrier density at transparency	1.4×10^{24} m^{-3}
τ_L	round-trip time in internal cavity	8 ps
τ_N	carrier lifetime	2.04 ns
τ_p	photon lifetime	1.927 ps
T	delay coupling time	1.001 ns
J_{th}	threshold current density	9.892×10^{32} $m^{-3}s^{-1}$
J	injection carrier rate	$1.44J_{th}$
f	free-running laser frequency	1.951×10^{14} Hz
Δf	frequency detuning between SLs	−40 GHz–40 GHz
k_c	mutual coupling strength	$0-50\,ns^{-1}$

where the integer j satisfies the following inequalities:

$$\begin{cases} \sum_{i=1}^{j} \lambda_i > 0 \\ \sum_{i=1}^{j+1} \lambda_i < 0 \end{cases} \tag{7}$$

After normalizing and linearizing Eqs. (1)–(3), Lyapunov spectrum can be calculated by adopting the method proposed in [33]. Table 1 is a list of used parameter values during the simulations, where for simplicity the parameters of SL1 and SL2 are assumed to be identical except the coupling strength and the frequency detuning between the two SLs are variable within a finite range.

3. Results and Discussion

3.1 Parameter Region Required for Chaotic Output

Maximum Lyapunov exponent (MLE) is one of the most important measures for the stability of nonlinear dynamical systems, and the existence of a positive MLE is one of widely acceptable evidences of deterministic chaos. MLE can be obtained based on rate equations of a dynamical system or with the help of experimentally measured time series [33], [43], [44]. Here, based on Eqs. (1)–(3), after numerically calculating the time series by MATLAB, the method proposed in [33] is adopted to extract MLE. Fig. 2 shows bifurcation diagrams and corresponding MLE of SL1 and SL2 as a function of mutual coupling strength. For $k_c < 2.7\,ns^{-1}$, the MLE is negative or close to zero, which correspond to the regions of steady-state, periodic oscillations, or quasi-periodic oscillations. With the increase of k_c from $2.7\,ns^{-1}$, MLE becomes positive and increases gradually, which demonstrates that both the two SLs enter chaotic states.

Besides coupling strength k_c, frequency detuning Δf is another key parameter to determine dynamical states of MDC-SLs. In order to specify the parameter region in which MDC-SLs operate at chaotic states, maps of MLE in the parameter space of k_c and Δf are displayed in Fig. 3, where different color characterizes different value of MLE. From this diagram, the upper boundary of the non-chaotic region (dark blue) for SL1 (SL2) presents a clear shapes as the Letter 'V' but show

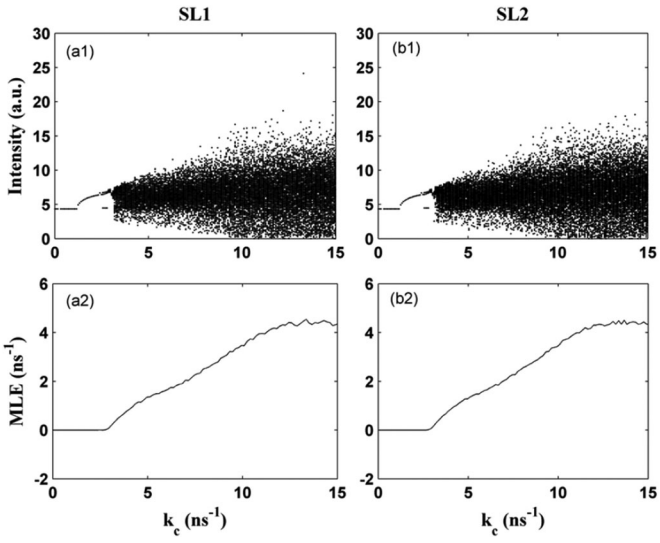

Fig. 2. Bifurcation diagrams (upper row) and MLE values (below row) as a function of the mutual coupling strength k_c under $\Delta f = 0$ GHz.

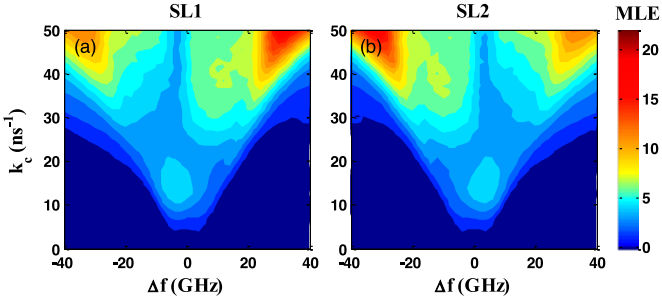

Fig. 3. Evolution maps of MLE values in the parameter space of the mutual coupling strength k_c and frequency detuning Δf.

a slightly asymmetrical feature to the frequency detuning. The region above the boundary of the Letter 'V', SL1 (SL2) behave chaotic oscillation. Moreover, through observing this diagram carefully, a mirror symmetry relationship can be found between the evolution maps of SL1 and SL2. That is to say, the left part of SL1's maps is similar to the right part of SL2's maps meanwhile the right part of SL1's maps is similar to the left part of SL2's maps, which is originated from the structural mirror symmetry being described by Eqs. (1)–(2).

3.2 Parameter Region for Generating Weak TDS Chaotic Signals

By using the fourth order Runge-Kutta algorithm, Eqs. (1)–(3) is normalized and numerically solved, and then the time series outputs from SL1 and SL2 can be obtained, Furthermore, corresponding ACFs can be calculated. In Fig. 4, the time series and corresponding ACFs are depicted for $(\Delta f, k_c) = (0, 27\,\mathrm{ns}^{-1})$ (the upper two rows) and $(\Delta f, k_c) = (0, 12\,\mathrm{ns}^{-1})$ (the below two rows), respectively. As shown in this diagram, both the two time series outputs from SL1 and SL2 are chaotic signals, but the chaotic temporal waveforms are quite different even if the two SLs are set by the same parameters. The reason is that, in a MDC-SLs configuration, the synchronization solution is unstable, and slight disturbances will make two SLs finally export two different waveforms. As a result, such MDC-SLs system possesses the superiority for simultaneously generating two sets

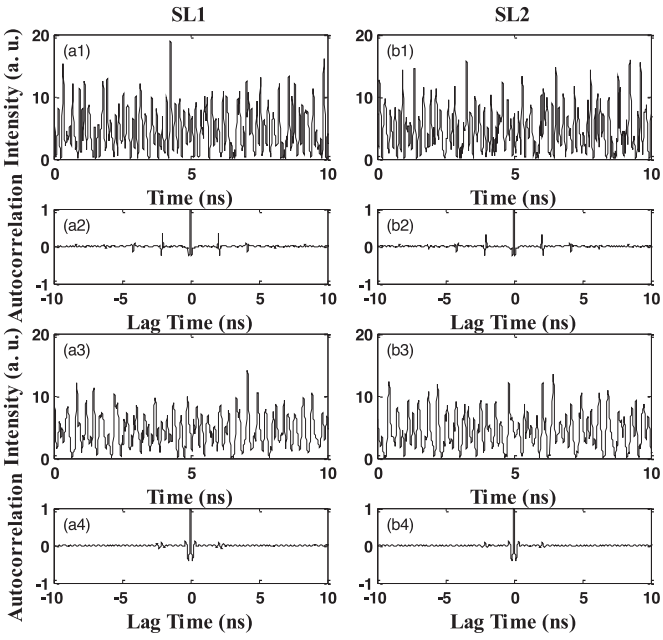

Fig. 4. Time series of MDC-SLs system and corresponding ACF for SL1 and SL2. The upper two rows are for $(\Delta f,\ k_c) = (0,\ 27\,ns^{-1})$ and the below two rows are for $(\Delta f,\ k_c) = (0,\ 12\ ns^{-1})$, respectively.

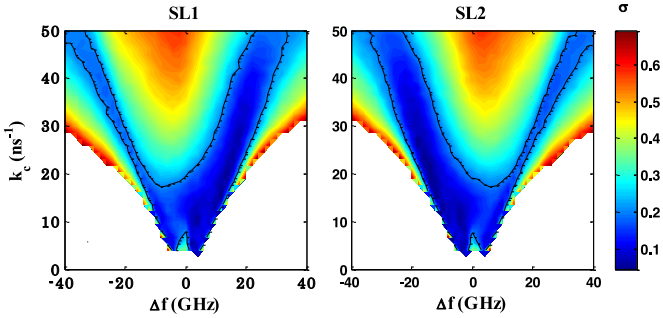

Fig. 5. Maps of the TDS in the parameter space of k_c and Δf. The black lines are marked for $\sigma = 0.2$, and the white region corresponds non-chaotic state.

of chaotic signals. However, the ACF for SL1 is similar to that for SL2. The reason is that, as demonstrated by our previous work [26], there exists a mirror symmetry relationship between the evolution maps of SL1 and SL2 with respect to frequency detuning. As a result, for $\Delta f = 0$, the ACF evolutions for SL1 and SL2 behave similar. Although it seems difficult to extract TDS directly from the chaotic waveforms [see Fig. 4(a1) and (b1)], the delay coupling time can still be clearly extracted from the peak locations by ACF [see Fig. 4(a2) and (b2)] when $(\Delta f,\ k_c) = (0,\ 27\,ns^{-1})$. However, for $(\Delta f,\ k_c) = (0, 12\,ns^{-1})$, the delay coupling time is difficult to extract from ACF since the TDS is very weak. Therefore, the TDS can be suppressed efficiently through selecting suitable parameters. In the following discussion, we define the amplitude σ to characterize whether the TD signature is obvious or not. The amplitude σ is the maximum ACF peak within a Δt of [1.6 ns, 2.4 ns].

In order to investigate thoroughly the influences of k_c and Δf on the TDS of chaotic signals, Fig. 5 shows the evolution maps of the TDS in the parameter space of k_c and Δf. The black lines are

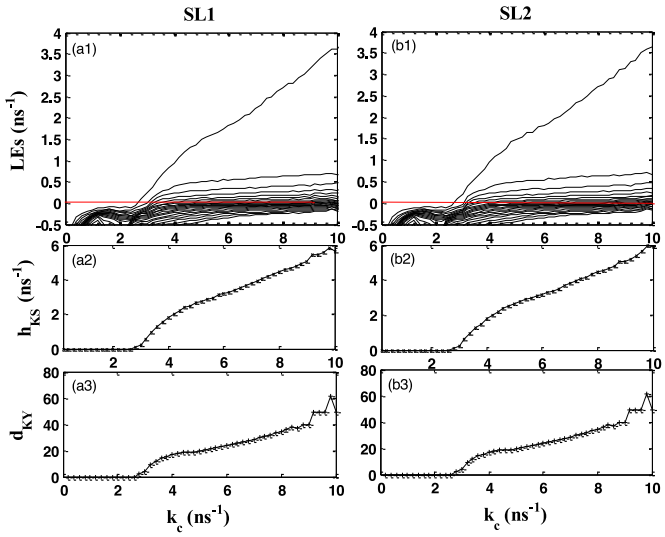

Fig. 6. LEs, KS entropy and KY dimension as a function of k_c under $\Delta f = 0$ GHz.

marked for $\sigma = 0.2$, and $\sigma < 0.2$ is regarded as a rough criterion to chaotic signals with weak TDS. Similar to Fig. 3, the mirror symmetry relationship is still existed between the two results for SL1 and SL2. When k_c is relatively low ($3\,\text{ns}^{-1} \leq k_c \leq 18\,\text{ns}^{-1}$) and meanwhile Δf varies in the range of -16 GHz $\leq \Delta f \leq 16$ GHz, the σ values are very small for two sets of chaotic signals. Under this case, two sets of chaotic signals with weak TDS can be obtained simultaneously. Next, we will emphatically analyze the complexity of generated chaotic signals under the case of $3\,\text{ns}^{-1} \leq k_c \leq 18\,\text{ns}^{-1}$ and -16 GHz $\leq \Delta f \leq 16$ GHz with the aim to acquiring chaotic signals with both weak TDS and high complexity.

3.3 Parameter Region for Generating Chaotic Signals With Both Weak TDS and High Complexity

As mentioned above, in order to calculate KS entropy and KY dimension, the first step is to calculate Lyapunov spectrum. Fig. 6 exhibits the 30 largest Lyapunov exponents (LEs), KS entropy (h_{KS}) and KY dimension (d_{KY})as a function of k_c for Δf is set at 0 GHz. As shown in this diagram, the MDC-SLs system possesses hyperchaotic behavior once $k_c > 3.2\,\text{ns}^{-1}$ since there exist more than one positive LE. With the increase of k_c from $2.6\,\text{ns}^{-1}$ to $10\,\text{ns}^{-1}$, all LEs and the number of positive LEs increase, which is a typical feature for time-delay dynamical systems [27], [45]. Accordingly, h_{KS} and d_{KY} for both two SLs increase with the increase of k_c. Additionally, the variation trends of h_{KS} and d_{KY} are similar for both two SLs, which is due to that the roles of the two SLs can be interchanged for $\Delta f = 0$. Certainly, for Δf takes other values except 0, the obtained results for SL1 will be different from that for SL2.

Next, we will analyze how Δf affects the complexity of chaotic signals generated by the MDC-SLs system. Fig. 7 simulates the 60 largest LEs, h_{KS} and d_{KY} as a function of Δf for $k_c = 9\,\text{ns}^{-1}$. As shown in Fig. 7(a1) and (b1), the variation of LEs with Δf is complex, and relatively small $|\Delta f|$ is helpful for generating chaotic signal with much more positive LEs. For -10GHz $\leq \Delta f \leq 10$ GHz, the two lasers simultaneously be have hyperchaotic (more than one positive LE). Combining Fig. 7(a2, b2) and (a3, b3), one can observe clearly that the mirror symmetry relationship between SL1 and SL2 also exists. Moreover, the chaotic signal output from the SL with a lower oscillation frequency possesses relative high h_{KS} and d_{KY}. For $k_c = 9\,\text{ns}^{-1}$, the peak location emerges at about $\Delta f = -5$ GHz for SL1 and about $\Delta f = 5$ GHz for SL2, respectively.

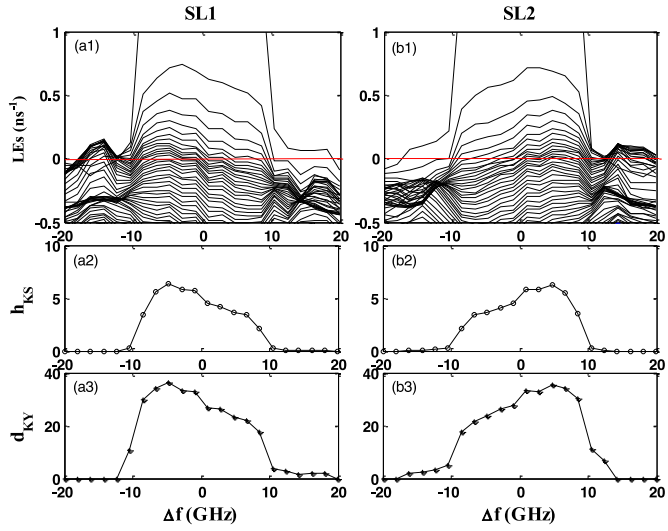

Fig. 7. LEs, KS entropy and KY dimension as a function of Δf under $k_c = 9\,\mathrm{ns}^{-1}$.

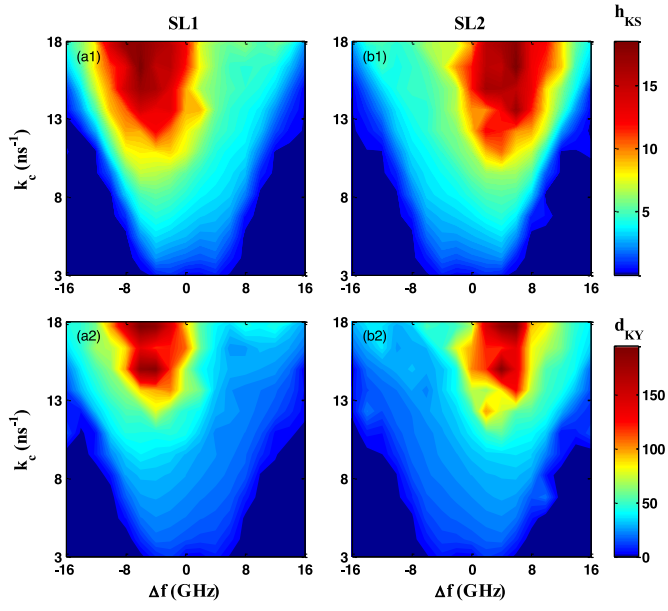

Fig. 8. Evolution maps of KS entropy (upper row) and KY dimension (below row) in the parameter space of k_c and Δf.

Finally, in Fig. 8, the evolution maps of KS entropy and KY dimension are displayed within the parameter space of $3\,\mathrm{ns} - 1 \leq k_c \leq 18\,\mathrm{ns}^{-1}$ and $-16\mathrm{GHz} \leq \Delta f \leq 16$ GHz, in which all the generated chaotic signals have weak TDS values. Here, different pseudo-color characterizes different value of h_{KS} or d_{KY}. From this diagram, one can see that h_{KS} and d_{KY} show similar evolution trend. Though it is impossible to generate simultaneously two sets of chaotic signals with the highest complexity(whose complexities take their maxima) due to mirror symmetry relationship of the MDC-SLs system, two sets of high quality chaotic signals with weak TDS and very high complexity can still be generated simultaneously within the optimal parameter region of $13\,\mathrm{ns}^{-1} < k_c \leq 18\,\mathrm{ns}^{-1}$ and Δf near 0 GHz.

By the way, it should be pointed out that though this research is based on DFB-SLs, for other SLs such as vertical-cavity surface-emitting laser (VCSELs) or quantum dot lasers (QDLs) similar analysis can also be conducted by modifying rate equations.

4. Conclusion

In summary, we have conducted a detailed simulation investigation on the high quality chaotic signal generation in a MDC-SLs system, where the TDS and complexity are adopted as two vital measures to assess the quality of generated chaotic signals. TDS is identified by autocorrelation function (ACF) while the complexity is evaluated by Kolmogorov-Sinai (KS) entropy and Kaplan-York (KY) dimension. Via by time series analysis and TDS extraction, the parameter space composed of the mutual coupling strength k_c and frequency detuning Δf is firstly determined for generating two sets of chaotic signals with low TDS. As a result, by further simulating KS entropy and KY dimension of chaotic signals, some optimal parameter regions for simultaneously generating two sets of high quality chaotic signals with both low TDS and high complexity have been specified. We believe that this work would be helpful for high quality chaotic carrier generation and its related applications.

References

[1] G. D. VanWiggeren and R. Roy, "Communication with chaotic lasers," *Science*, vol. 279, no. 5354, pp. 1198–1200, Feb. 1998.

[2] A. Argyris *et al.*, "Chaos-based communications at high bit rates using commercial fibre-optic links," *Nature*, vol. 438, no. 7066, pp. 343–346, Nov. 2005.

[3] Y. H. Hong, W. L. Min, and K. A. Shore, "Optimised message extraction in laser diode based optical chaos communications," *IEEE J. Quantum Electron.*, vol. 46, no. 2, pp. 253–257, Dec. 2010.

[4] N. Jiang, J. Wang, D. Liu, C. Xue, and K. Qiu, "Secure WDM-PON based on chaos synchronization and subcarrier modulation multiplexing," *J. Opt. Soc. Amer. B*, vol. 33, no. 4, pp. 637–642, Mar. 2016.

[5] I. Reidler, Y. Aviad, M. Rosenbluh, and I. Kanter, "Ultrahigh-speed random number generation based on a chaotic semiconductor laser," *Phys. Rev. Lett.*, vol. 103, no. 2, Jul. 2009, Art. no. 024102.

[6] I. Kanter, Y. Aviad, I. Reidler, E. Cohen, and M. Rosenbluh, "An optical ultrafast random bit generator," *Nature Photon.*, vol. 4, no. 1, pp. 58–61, Dec. 2010.

[7] X. Tang *et al.*, "Tbits/s physical random bit generation based on mutually coupled semiconductor laser chaotic entropy source," *Opt. Exp.*, vol. 23, no. 26, pp. 33130–33141, Dec. 2015.

[8] P. Li *et al.*, "Fully photonics-based physical random bit generator," *Opt. Lett.*, vol. 41, no. 14, pp. 3347–3350, Jul. 2016.

[9] F. Y. Lin and J. M. Liu, "Chaotic lidar," *IEEE J. Sel. Topics Quantum Electron.*, vol. 10, no. 5, pp. 991–997, Dec. 2004.

[10] S. L. Yan, "Chaotic synchronization of two mutually coupled semiconductor lasers for optoelectronic logic gates," *Commun. Nonlinear Sci. Numer. Simul.*, vol. 17, no. 7, pp. 2896–2904, Jul. 2012.

[11] D. Rontani, A. Locquet, M. Sciamanna, D. S. Citrinm, and S. Ortin, "Time-delay identification in a chaotic semiconductor laser with optical feedback: A dynamical point of view," *IEEE J. Quantum Electron.*, vol. 45, no. 7, pp. 879–891, Jun. 2009.

[12] D. Rontani, A. Locquet, M. Sciamanna, and D. S. Citrin, "Loss of time-delay signature in the chaotic output of a semiconductor laser with optical feedback," *Opt. Lett.*, vol. 32, no. 20, pp. 2960–2962, Jul. 2007.

[13] V. S. Udaltsov, J. P. Goalgcbucr, L. Largcr, J. B. Cucnot, P. Lcvy, and W. T. Rhodcs, "Cracking chaos-based encryption systems ruled by nonlinear time delay differential equations," *Phys. Lett. A*, vol. 308, no. 1, pp. 54–60, Feb. 2003.

[14] A. Uchida *et al.*, "Fast physical random bit generation with chaotic semiconductor lasers," *Nature Photon.*, vol. 2, no. 12, pp. 728–732, Nov. 2008.

[15] A. Elsonbaty, S. F. Hegazy, and S. S. A. Obayya, "Simultaneous suppression of time-delay signature in intensity and phase of dual-channel chaos communication," *IEEE J. Quantum Electron.*, vol. 51, no. 9, Sep. 2015, Art. no. 2400309.

[16] H. Lin, A. Khurram, and Y. H. Hong, "Time-delay signatures in multi-transverse mode VCSELs subject to double-cavity polarization-rotated optical feedback," *Opt. Commun.*, vol. 377, pp. 128–138, Oct. 2016.

[17] N. Q. Li, W. Pan, A. Locquet, and D. S. Citrin, "Time-delay concealment and complexity enhancement of an external-cavity laser through optical injection," *Opt. Lett.*, vol. 40, no. 19, pp. 4416–4419, Sep. 2015.

[18] M. W. Lee, P. Rees, K. A. Shore, S. Ortin, L. Pesquera, and A. Valle, "Dynamical characterisation of laser diode subject to double optical feedback for chaotic optical communications," *IEE Proc.-Optoelectron.*, vol. 152, no. 2, pp. 97–102, Apr. 2005.

[19] J. Zhang, C. Feng, M. Zhang, Y. Liu, and Y. Zhang, "Suppression of time delay signature based on Brillouin backscattering of chaotic laser," *IEEE Photon. J.*, vol. 9, no. 2, Apr. 2017, Art. no. 1502408.

[20] X. Zhu *et al.*, "An optically coupled electro-optic chaos system with suppressed time-delay signature," *IEEE Photon. J.*, vol. 9, no. 3, Jun. 2017, Art. no. 6601009.

[21] S. S. Li, Q. Liu, and S. C. Chan, "Distributed feedbacks for time-delay signature suppression of chaos generated from a semiconductor laser," *IEEE Photon. J.*, vol. 4, no. 5, pp. 1930–1935, Oct. 2012.

[22] J. G. Wu *et al.*, "Time delay signature concealment of optical feedback induced chaos in an external cavity semiconductor laser," *Opt. Exp.*, vol. 18, no. 7, pp. 6661–6666, Mar. 2010.
[23] Z. Q. Zhong, Z. M. Wu, and G. Q. Xia, "Experimental investigation on the time-delay signature of chaotic output from a 1550 nm vcsel subject to FBG feedback," *Photon. Res.*, vol. 5, no. 1, pp. 6–10, Dec. 2017.
[24] J. G. Wu, G. Q. Xia, and Z. M. Wu, "Suppression of time delay signatures of chaotic output in a semiconductor laser with double optical feedback," *Opt. Exp.*, vol. 17, no. 22, pp. 20124–20133, Oct. 2009.
[25] J. G. Wu *et al.*, "Simultaneous generation of two sets of time delay signature eliminated chaotic signals by using mutually coupled semiconductor lasers," *IEEE Photon. Technol. Lett.*, vol. 23, no. 12, pp. 759–761, Mar. 2011.
[26] J. G. Wu, Z. M. Wu, G. Q. Xia, and G. Y. Feng, "Evolution of time delay signature of chaos generated in a mutually delay-coupled semiconductor lasers system," *Opt. Exp.*, vol. 20, no. 2, pp. 1741–1753, Jan. 2012.
[27] R. Vicente, J. Dauden, P. Colet, and R. Torah, "Analysis and characterization of the hyperchaos generated by a semiconductor laser subject to a delayed feedback loop," *IEEE J. Quantum Electron.*, vol. 41, no. 4, pp. 541–548, Apr. 2005.
[28] K. M. Short and A. T. Parker, "Unmasking a hyperchaotic communication scheme," *Phys. Rev. E*, vol. 58, no. 1, pp. 1159–1162, Jul. 1998.
[29] T. Yang, "A survey of chaotic secure communication systems," *Int. J. Comput. Cognit.*, vol. 2, no. 2, pp. 81–130, Jun. 2004.
[30] J. D. Farmer, "Chaotic attractors of an infinite-dimensional system," *Physica D*, vol. 4, no. 3, pp. 366–393, Mar. 1982.
[31] C. Barbara and C. Silvano, "Hyperchaotic behavior of two bidirectionally Chua's circuits," *Int. J. Circuit Theory Appl.*, vol. 30, no. 6, pp. 625–637, Sep. 2002.
[32] S. Xiang *et al.*, "Quantifying chaotic unpredictability of vertical-cavity surface-emitting lasers with polarized optical feedback via permutation entropy," *IEEE J. Sel. Topics Quantum Electron.*, vol. 17, no. 5, pp. 1212–1219, Sep./Oct. 2011.
[33] A. Uchida, *Optical Communication With Chaotic Lasers, Applications of Nonlinear Dynamics and Synchronization*. Weinheim, Germany: Wiley-VCH, 2012.
[34] T. Heil, I. Fischer, W. Elsasser, J. Muler, and C. R. Mirasso, "Chaos synchronization and spontaneous symmetry-breaking in symmetrically delay-coupled semiconductor lasers," *Phys. Rev. Lett.*, vol. 86, no. 5, pp. 795–798, Jan. 2001.
[35] R. López-Ruiz, H. L. Mancini, and X. Calbet, "A statistical measure of complexity," *Phys. Lett. A*, vol. 209, nos. 5–6, pp. 321–326, Dec. 1995.
[36] M. T. Martin, A. Plastino, and O. A. Rosso, "Generalized statistical complexity measures: Geometrical and analytical properties," *Physica A*, vol. 369, no. 2, pp. 439–462, Sep. 2006.
[37] C. Bandt and B. Pompe, "Permutation entropy: a natural complexity measure for time series," *Phys. Rev. Lett.*, vol. 88, no. 17, Apr. 2002, Art. no. 174102.
[38] L. Zunino, M. C. Soriano, I. Fischer, O. A. Rosso, and C. R.Mirasso, "Permutation-information-theory approach to unveil delay dynamics from time-series analysis," *Phys. Rev. E*, vol. 82, no. 4, Oct. 2010, Art. no. 046212.
[39] M. C. Soriano, L. Zunino, O. A. Rosso, I. Fischer, and C. R. Mirasso, "Time scales of a chaotic semiconductor laser with optical feedback under the lens of a permutation information analysis," *IEEE J. Quantum Electron.*, vol. 47, no. 2, pp. 252–261, Jan. 2011.
[40] P. W. Lamberti, M. T. Martin, A. Plastino, and O. A. Rosso, "Intensive entropic non-triviality measure," *Physica A*, vol. 334, nos. 1–2, pp. 119–131, Mar. 2004.
[41] K. E. Chlouverakis, A. Argyris, A. Bogris, and D. Syvridis, "Complexity and synchronization in chaotic fiber-optic systems," *Physica D*, vol. 237, no. 4, pp. 568–572, Apr. 2008.
[42] K. Pyragas, "Synchronization of coupled time-delay systems: Analytical estimations," *Phys. Rev. E*, vol. 58, no. 3, pp. 3067–3071, Sep. 1998.
[43] M. T. Rosenstein, J. J. Collins, and C. J. De Luca, "A practical method for calculating largest Lyapunov exponents from small data sets," *Physica D*, vol. 65, nos. 1–2, pp. 117–134, May 1993.
[44] A. Wolf, J. B. Swift, H. L. Swinney, and J. A. Vastano, "Determing Lyapunov exponent from a time series," *Physica D*, vol. 16, no. 3, pp. 285–317, Jul. 1985.
[45] A. Namajūnas, K. Pyragas, and A. Tamaševičius, "An electronic analog of the Mackey-glass system," *Phys. Lett. A*, vol. 201, no. 1, pp. 42–46, May 1995.